Effect of Percolation on Structural and Electrical Properties of MIC Processed SiGe/Al Multilayers

M. LINDORF,[1,4] H. ROHRMANN,[2] G. SPAN,[3] and M. ALBRECHT[1]

1.—Institute of Physics, University of Augsburg, Universitätsstraße 1, 86159 Augsburg, Germany. 2.—Evatec Advanced Technologies AG, Iramali 18, 9496 Balzers, Liechtenstein. 3.—O-Flexx Technologies GmbH, Auf der Höhe 49, 47059 Duisburg, Germany. 4.—e-mail: marc.lindorf@physik.uni-augsburg.de

The effect of metal induced crystallization (MIC) is widely used in the production of electronic devices by forming large grained polycrystalline Si from amorphous Si in contact with Al. This effect can also be utilized in conjunction with silicon-germanium (SiGe) alloys and thus provides means of a possible low cost production of future high temperature thermoelectric devices. In this work, sputter deposited multilayer systems of $Si_{80}Ge_{20}$/Al thin films have been investigated. The effect of MIC is used to crystallize the initially amorphous SiGe while simultaneously doping it with Al. As metallic phases would be detrimental to the thermoelectric performance, special interest is directed to the Al layers and their dissociation during the annealing treatment. A percolation limit regarding the thickness and continuity of the Al layers was found, but no detrimental side effects with respect to the MIC process could be detected.

Key words: Thermoelectric, silicon germanium, aluminum, metal induced crystallization, percolation

INTRODUCTION

Silicon-germanium (SiGe) alloys are well known thermoelectric materials suited for high temperature application around 873–1273 K.[1] During the last decade, strong interest for this classical thermoelectric material got reignited due to the concepts of increasing the dimensionless figure-of-merit $ZT = S^2\sigma\kappa^{-1}T$ by nanostructuring and therefore decoupling the Seebeck coefficient S, electrical conductivity σ, and thermal conductivity κ.[2,3] One approach in this respect aims for the introduction of grain boundaries in the nanometer range, which are able to scatter phonons effectively, decreasing the lattice contribution of the thermal conductivity[3,4] or by increasing the Seebeck coefficient via energyfiltering.[2,5] Similar structures have already been fabricated with help of the so called effect of metal induced crystallization (MIC) for silicon based solar cells and electronic devices.[6] MIC is a diffusion driven process, lowering the crystallization temperature of amorphous semiconductors, being in contact with a crystalline metal.[7] The effect of MIC is also applicable to SiGe enabling low cost production of polycrystalline, doped SiGe thin films.[8–10] A multilayer structure of multiple $Si_{80}Ge_{20}$/Al stacks was chosen for this work to ensure SiGe grain sizes in the nanometer range after annealing by impinging the grain growth among each of the individual layers. Since metallic phases like pure Al have very low thermoelectric efficiencies, it is important to completely dissociate the Al layers during the diffusion driven MIC process. Therefore, rather thin Al layers were chosen to facilitate the dissociation of the Al layers.

EXPERIMENTAL PROCEDURES

Two samples of SiGe/Al multilayers were prepared by magnetron sputter deposition at room temperature on low temperature cofired ceramic (LTCC) substrates. The samples consisted of 100 bilayers of $Si_{80}Ge_{20}$(100 Å)/Al(10 Å) or 50 bilayers of

$Si_{80}Ge_{20}$(400 Å)/Al(40 Å). For the deposition of SiGe, a $Si_{80}Ge_{20}$ alloy sputter target was used.

All deposited films are amorphous and underwent an annealing procedure in a quartz glass tube furnace at 873 K for 1 h to induce MIC. The annealing was performed under vacuum (~1000 Pa) with a flow of dry N_2 for oxidation protection. Structural investigations were carried out with a JEOL 2100 F transmission electron microscope (TEM) at 200 kV. The structural properties of the samples were analyzed using a 3003 PTS x-ray diffractometer from Seifert with Cu-K_α radiation (λ = 1.5405 Å). The x-ray diffraction (XRD) patterns were measured in θ–2θ mode using a scan speed of 8 s/step and a step size of 0.05°. The specific electrical resistivity ρ was measured in the temperature range of 300–750 K with a home-built system, operating at pressures below 10^{-4} Pa. Samples of size 1×1 cm^2 were utilized in van-der-Pauw geometry for resistance measurements. For calculation of ρ the nominal combined thickness of all SiGe layers was used as TEM imaging was in agreement to the actual observed SiGe layer thickness for all samples.

Samples in the following will be addressed by codenaming: First the used substrate will be given, second the SiGe and Al interlayer thickness d_{SiGe} and d_{Al} (in units of Å), respectively, and last the annealing temperature in units of K (if applied). Hence, the sample deposited on LTCC with 100 Å of SiGe and 10 Å of Al interlayer thickness annealed at 873 K is named LTCC-100SiGe-10Al-873 K.

RESULTS AND DISCUSSION

In the as-deposited state two distinctive types of the SiGe-Al structure are observed by TEM. In the case of the thicker sample with an Al layer thickness of 40 Å, continuous layers in multilayer structure are observed in Fig. 1b. Contrary to this, the thinner sample with an Al layer thickness of 10 Å exhibits an assembly of Al nanodots as shown in Fig. 1a. Additionally, it is apparent for both samples that the Al layers appear darker than the remaining parts of the sample. With a layer thickness ratio of $d_{Al}/d_{SiGe} = 0.1$, the majority of the samples is expected to be SiGe and to appear darker in a TEM bright field image due to higher average atomic mass compared to Al. Nonetheless, the Al parts reveal darker contrast in comparison. This contradiction is solved in Fig. 2, where a high resolution image of the nanodots of sample LTCC-100SiGe-10Al is presented. Lattice planes are distinguishable in the nanodots, corresponding to crystalline Al and such added diffraction contrast makes the Al appear darker than the SiGe.

The specific electrical resistance ρ was measured *in situ* during annealing up to temperatures of 750 K in our home-built system for both samples and is displayed in Fig. 3. Sample LTCC-100SiGe-10Al shows high electrical resistance of $\rho > 10^0$ Ωm in the as-deposited state, because the electric transport is governed by the amorphous SiGe matrix surrounding the Al nanodots. The electrical resistance decreases slowly with temperature and exhibits a steep drop of three orders of magnitude for temperatures above 650 K. For cooling down ρ maintains its lowered value while showing a negative temperature coefficient typical for crystalline semiconductors. Please note that the power supply used in our measurement system was operating near its maximum load for such high resistances at the beginning of the annealing process and thus it was difficult to determine if stable contacts were obtained. Therefore, the kinks observed in Fig. 3a are most likely due to the sample contacts.

Sample LTCC-400SiGe-40Al has very low electrical resistance in the as-deposited state of $\rho = 2 \times 10^{-5}$ Ωm. The electrical resistance increases slowly with temperature, indicating metallic transport behavior via the continuous Al layers in the sample. For temperature above 450 K, ρ starts to increase strongly until a maximum in electrical resistance is reached for a temperature of 530 K. Afterwards a decrease in ρ similar to the other sample is observed. Finally, an electrical resistance in the range between 18×10^{-5} Ωm and 9×10^{-5} Ωm with a negative temperature coefficient is achieved, indicating again semiconductor-like behavior.

The change in electrical resistance observed for both samples is attributed to the effect of MIC. For the thin-layered sample a steep decrease in ρ is observed as the SiGe crystallizes and is doped by Al during MIC. Thus the sample changes from amorphous to crystalline, Al-doped semiconducting SiGe. In case of the thick-layered sample an intermediate maximum in resistance is observed. First the electrical current is carried by continuous Al layers, which start to diffuse at elevated temperatures due to MIC. Concurrently, the SiGe starts to crystallize and such a competing process is started, where ρ on the one hand is increased due to the dissolving of the Al layers and on the other hand is decreased to the ongoing crystallization of SiGe. Furthermore, the transition temperature for the crystallization of SiGe was higher for the sample with thinner Al layers and thus the increased electrical resistance for the thin-layered sample after the annealing cycle can be explained by incomplete crystallization. A similar behavior has already been reported in the literature.[11,12]

Furthermore, XRD was conducted on both samples in the as-deposited state and after annealing at 873 K for 1 h. The respective diffraction patterns are shown in Fig. 4. Only substrate related peaks are visible in the as-deposited state. Both annealed samples reveal diffraction peaks near the theoretical expected value of crystalline $Si_{80}Ge_{20}$ estimated by Vegard's law.[13] A shift to higher angles is detected, indicating a slight surplus of Si. The crystallization temperature of SiGe is reported to be around 930 K varying with composition and

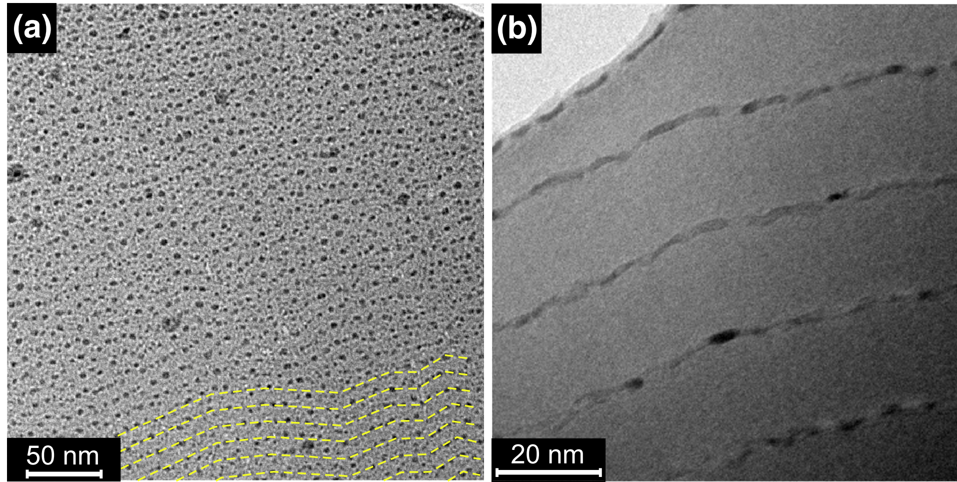

Fig. 1. TEM bright field cross section images of samples (a) LTCC-100SiGe-10Al and (b) LTCC-400SiGe-40Al in the as-deposited state. For the thick-layered sample continuous Al layers are observed, while for the thin-layered sample an assembly of Al nanodots is present. Dashed lines indicate the growth direction for the thin-layered sample.

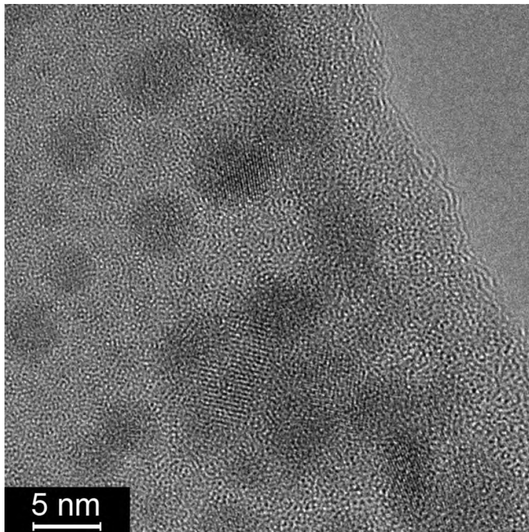

Fig. 2. TEM bright field cross section image of sample LTCC-100SiGe-10Al in the as-deposited state taken at high resolution. Lattice planes are distinguishable for the Al nanodots, explaining the darker contrast due to added diffraction contrast of the crystalline Al.

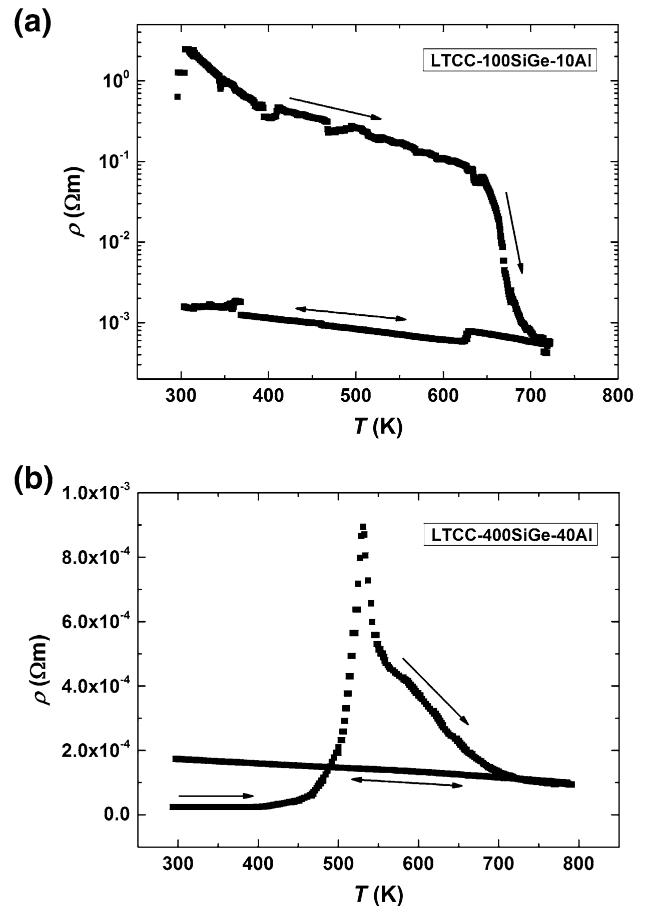

Fig. 3. *In situ* measurement of the specific electrical resistance ρ for samples (a) LTCC-100SiGe-10Al and (b) LTCC-400SiGe-40Al starting in the as-deposited state. Both samples show a change in resistance during heating due to the effect of MIC.

annealing conditions.[14] Hence the detection of diffraction peaks of crystalline $Si_{80}Ge_{20}$ and the irreversible changes in electrical resistance for annealing below the typical crystallization temperature of $Si_{80}Ge_{20}$ are evidence to the effect of MIC in both samples.

The specific electrical resistance of both annealed samples was also measured and is shown in Fig. 5. The semiconducting transport character becomes apparent again as a negative temperature coefficient is observed for both samples. Additionally, the electrical resistance of sample LTCC-100SiGe-10Al is reduced by a factor of 2 compared to the achieved resistance after *in situ* annealing at 750 K. As the electrical resistance of sample LTCC-400SiGe-40Al is still lower by a factor of two compared to LTCC-100SiGe-10Al after annealing at 873 K, this again hints to an incomplete crystallization process for sample LTCC-100SiGe-10Al.

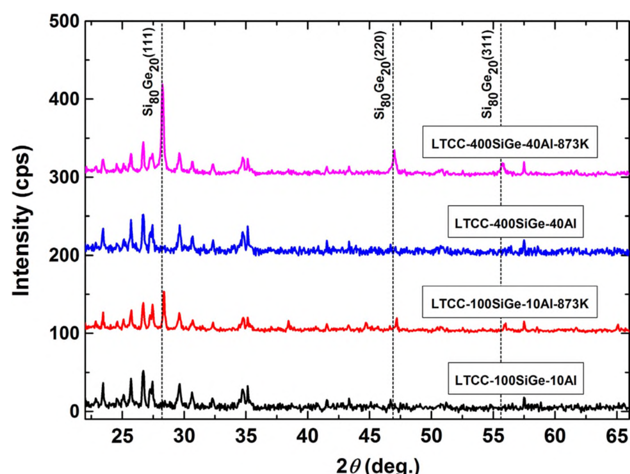

Fig. 4. Comparison of diffraction patterns of samples in as-deposited state and after annealing at 873 K for 1 h.

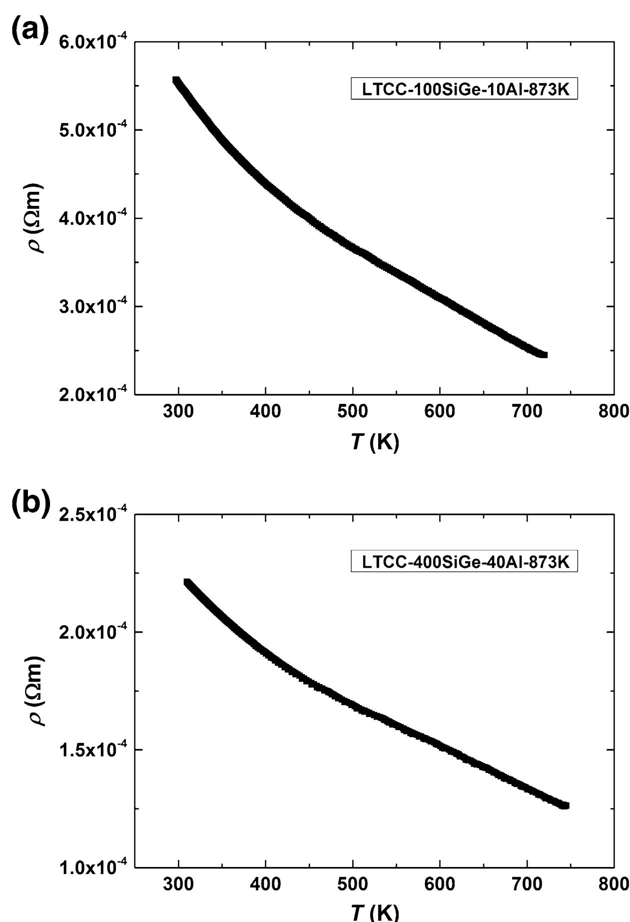

Fig. 5. Specific electrical resistance ρ of samples (a) LTCC-100SiGe-10Al and (b) LTCC-400SiGe-40Al measured after annealing at 873 K for 1 h.

CONCLUSION

Two different multilayers of $[Si_{80}Ge_{20}(100\ \text{Å})/Al(10\ \text{Å})]_{100}$ and $[Si_{80}Ge_{20}(400\ \text{Å})/Al(40\ \text{Å})]_{50}$ were prepared via sputter deposition onto LTCC substrates. The as-deposited thick-layered sample showed the expected multilayer structures of alternating, continuous SiGe and Al layers by TEM imaging. Contrary to that, the thin-layered sample exhibited no continuous Al layers, revealing an assembly of Al nanodot structures. For both samples, Al appeared to be in a crystalline state. In agreement to the observed different morphologies of Al, the samples exhibited metal-like and isolator-like specific electrical resistance in the as-deposited state. Heat treatment of the two samples led to a change in resistivity due to the effect of MIC at onset temperatures of 650 K (thin-layered sample) and 450 K (thick-layered sample). After this structural phase change, both samples showed semiconductor-like specific electrical resistances in the range of 10^{-4} to 10^{-3} Ωm. Diffraction patterns taken for the annealed samples (at 873 K, 1 h) revealed diffraction peaks, matching the values of crystalline $Si_{80}Ge_{20}$. Therefore, no detrimental effects to the MIC process could be detected with regard to the non-continuous Al layers except for an increased resistance, which could be attributed to a not completely finished crystallization process.

ACKNOWLEDGEMENTS

Financial support from the German Research Foundation (DFG) within the priority Program SPP 1386 and from the European Commission within the FP-7 Project NanoHiTEC (FP7-263306) is gratefully acknowledged.

REFERENCES

1. C.B. Vining, *CRC Handbook of Thermoelectrics*, ed. D.M. Rowe (Florida: Boca Raton, 1995), p. 329.
2. A.J. Minnich, M.S. Dresselhaus, Z.F. Ren, and G. Chen, *Energy Environ. Sci.* 2, 466 (2009).
3. Y. Lan, A.J. Minnich, G. Chen, and Z.F. Ren, *Adv. Funct. Mater.* 20, 357 (2010).
4. G.H. Zhu, H. Lee, Y.C. Lan, X.W. Wang, G. Joshi, D.Z. Wang, J. Yang, D. Vashaee, H. Guilbert, A. Pillitteri, M.S. Dresselhaus, G. Chen, and Z.F. Ren, *Phys. Rev. Lett.* 102, 196803 (2009).
5. T.H. Zou, X.Y. Qin, D. Li, B.J. Ren, G.L. Sun, Y.C. Dou, Y.Y. Li, L.L. Li, J. Zhang, and H.X. Xin, *J. Appl. Phys.* 115, 053710 (2014).
6. S. Ii, T. Hirota, K. Fujimoto, Y. Sugimoto, N. Takata, K. Ikeda, H. Nakashima, and H. Nakashima, *Mater. Trans.* 49, 723 (2008).
7. L.P.H. Jeurgens, Z. Wang, and E.J. Mittemeijer, *Int. J. Mater. Res.* 100, 1281 (2009).
8. R. Lechner, M. Buschbeck, M. Gjukic, and M. Stutzmann, *Phys. Status Solidi* 1, 1131 (2004).
9. H. Takiguchi, K. Fukui, and Y. Okamoto, *Jpn. J. Appl. Phys.* 49, 115602 (2010).
10. M. Kurosawa, N. Kawabata, T. Sadoh, and M. Miyao, *ECS J. Solid State Sci. Technol.* 1, 144 (2012).
11. Z.M. Wang, J.Y. Wang, L.P.H. Jeurgens, and E.J. Mittemeijer, *Phys. Rev. Lett.* 100, 125503 (2008).
12. T.J. Konno and R. Sinclair, *Philos. Mag. B* 66, 749 (1992).
13. J.P. Dismukes, L. Ekstrom, and R.J. Paff, *J. Phys. Chem.* 68, 3021 (1964).
14. C.-W. Hwang, M.-K. Ryu, K.-B. Kim, S.-C. Lee, and C.-S. Kim, *J. Appl. Phys.* 77, 3042 (1995).